JACS
JOURNAL OF THE AMERICAN CHEMICAL SOCIETY

Article

pubs.acs.org/JACS

Molecular Functionalization of Graphite Surfaces: Basal Plane versus Step Edge Electrochemical Activity

Guohui Zhang, Paul M. Kirkman, Anisha N. Patel, Anatolii S. Cuharuc, Kim McKelvey, and Patrick R. Unwin*

Department of Chemistry, University of Warwick, Coventry CV4 7AL, United Kingdom

Supporting Information

ABSTRACT: The chemical functionalization of carbon surfaces has myriad applications, from tailored sensors to electrocatalysts. Here, the adsorption and electrochemistry of anthraquinone-2,6-disulfonate (AQDS) is studied on highly oriented pyrolytic graphite (HOPG) as a model sp^2 surface. A major focus is to elucidate whether adsorbed electroactive AQDS can be used as a marker of step edges, which have generally been regarded as the main electroactive sites on graphite electrode surfaces. First, the macroscopic electrochemistry of AQDS is studied on a range of surfaces differing in step edge density by more than 2 orders of magnitude, complemented with ex situ tapping mode atomic force microscopy (AFM) data. These measurements show that step edges have little effect on the extent of adsorbed electroactive AQDS. Second, a new fast scan cyclic voltammetry protocol carried out with scanning electrochemical cell microscopy (SECCM) enables the evolution of AQDS adsorption to be followed locally on a rapid time scale. Subsequent AFM imaging of the areas probed by SECCM allows a direct correlation of the electroactive adsorption coverage and the actual step edge density of the *entire working area*. The amount of adsorbed electroactive AQDS and the electron transfer kinetics are independent of the step edge coverage. Last, SECCM reactive patterning is carried out with complementary AFM measurements to probe the diffusional electroactivity of AQDS. There is essentially uniform and high activity across the basal surface of HOPG. This work provides new methodology to monitor adsorption processes at surfaces and shows unambiguously that there is no correlation between the step edge density of graphite surfaces and the observed coverage of electroactive AQDS. The electroactivity is dominated by the basal surface, and studies that have used AQDS as a marker of steps need to be revised.

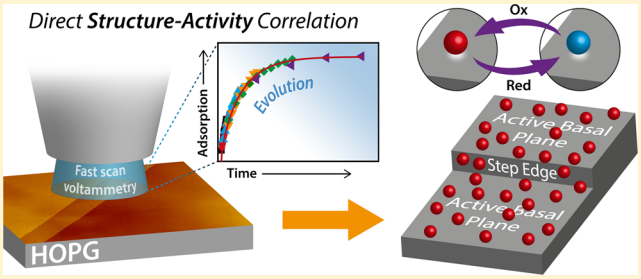

INTRODUCTION

Carbon offers a broad range of electrode materials for electrochemistry and electroanalysis and is particularly attractive where low background currents, a wide potential window, chemical inertness, and biocompatibility are desired.[1−4] Glassy carbon (GC), boron-doped diamond, and graphite have long received attention for electroanalytical and electrocatalytic measurements,[5−11] and more recently, carbon nanotubes and graphene have generated considerable interest.[12−17] However, despite well-defined bulk properties and structure, carbon materials can possess rather complex surface chemistry that may substantially impact the resulting electrochemistry.[6] Indeed, the range of functional groups present at different carbon electrode/electrolyte interfaces is yet to be fully understood[9] and is significantly impacted by electrode preparation.[18] Additionally, a range of surface chemical modifications of carbon materials are readily carried out.[19] Such protocols may provide a means of enhancing electrode performance, for example, by improving resistance to fouling, promoting electrocatalysis, suppressing the response of competing interfering species, or creating selectivity toward particular analytes.[20−23]

Surface modifications have also been proposed as a route to measure the quality of carbon electrode surfaces.[24,25] In particular, it has been suggested that the adsorption of redox-active organic molecules, such as quinones, can be used as a measure of the percentage of electrochemically active step edge sites present on graphite.[26,27] Quinones adsorb spontaneously onto a range of surfaces,[28−31] including carbon,[32,33] and readily undergo a $2e^-$ and $2H^+$ reduction in acidic aqueous media.[31,34−36] Studies of basal plane graphite[32,33] are particularly pertinent, in light of the considerable recent revision of, and interest in, the local electrochemical activity of highly oriented pyrolytic graphite (HOPG).[37−41]

Previous studies proposed that the step edge density on basal plane HOPG correlated with various electrochemical measurements in aqueous solution, specifically the double-layer capacitance ($C°$), the electron transfer kinetics for the redox couple ferri/ferrocyanide, and the surface coverage (Γ_{ads}) of adsorbed electroactive anthraquinone-2,6-disulfonate (AQDS).[26,27,42] These studies found that cleaved HOPG surfaces with greater step edge coverage tended to display

Received: May 26, 2014
Published: July 18, 2014

   dx.doi.org/10.1021/ja505266d | J. Am. Chem. Soc. 2014, 136, 11444−11451

higher Γ_{ads} for AQDS adsorption (at a particular bulk concentration). In turn, surfaces with higher Γ_{ads} also showed a higher standard rate constant, k_0, for ferri/ferrocyanide and higher C°. Hence, these easy to measure parameters became indirect proxies for determining the amount of step edge defects on an HOPG surface. However, the only attempt to correlate step edge density and Γ_{ads} focused on samples with a very narrow range of step densities (from 0.7 to 1.6%) with relatively high uncertainty in the absolute step edge density values.[26] Moreover, the ferri/ferrocyanide couple has since been shown to be problematic on the basal surface of graphite[41] and other surfaces.[43] These various issues, and further points outlined below, raise significant questions as to the validity of AQDS adsorption as a marker of step edge density and, more broadly, the veracity of older models of HOPG electrochemistry.

It is important to point out that the apparent correlation between the measured step edge coverage and AQDS adsorption required 30 times the step edge area than could be accounted for by the steps alone, and it was thus proposed that there was a pronounced electronic disturbance at step edges extending 5 nm from step edges (on the top terrace of the step),[26] with no electrochemistry on any other part of the basal surface. This was despite the fact that atomic force microscopy (AFM) imaging later indicated extensive multilayer surface coverage, resulting in a film with a high density of pinholes on the surface.[44] It was thus concluded that AQDS adsorption took place indiscriminately on the basal and step edge sites, but *only absorbed material at the step edges was electroactive*. However, recent scanning tunneling microscopy and spectroscopy studies have shown that the density of states (DOS) is more or less uniform across HOPG, being enhanced only over ca. 1 nm of zigzag step edges,[45−47] with little enhancement at armchair step edges, which are the dominant edge sites on graphite.[46,47] In fact, there is negligible effect of step edges on the overall DOS at the HOPG basal surface if terraces with zigzag edges are wider than 10 nm.[45,48] The step spacing is much greater than this for the overwhelming majority of HOPG samples used for electrochemistry, unless the surface was deliberately damaged by laser ablation.[27] This suggests that the macroscopic electrochemical measurements of basal plane HOPG should be independent of step edge density. This has been found recently for a diversity of electrochemical processes at HOPG surfaces with a wide range of step densities.[40,49,50] Moreover, microscopic and nanoscopic measurements have reported high intrinsic activity of the basal surface,[40,41,49,51−55] in contrast with the earlier literature, which proposed that the basal surface of HOPG was inert or largely inert.[56,57]

In this paper, we report detailed investigations of the adsorption and electrochemistry of AQDS on HOPG, with the particular goal of elucidating whether it is an appropriate measure for determining step edge density. More generally, this serves as an important model system to introduce new methodology for localized quantitative measurements of adsorption. To these ends, we use macroscopic voltammetry to measure adsorbed electroactive AQDS on freshly cleaved HOPG with high precision. By using four different HOPG grades with step edge densities spanning a range of more than 2 orders of magnitude, and using different cleavage methods, we are able to precisely elucidate the influence of step edge density on fractional coverage of electroactive material, Θ_{ads} (defined as Γ_{ads}/Γ_0, where Γ_{ads} is the surface coverage and Γ_0 is the theoretical maximum coverage). We find no correlation: Θ_{ads} *is independent of the grade of HOPG and cleavage method*. These key results are unequivocally confirmed with innovative fast scan cyclic voltammetry measurements using a new fast scan cyclic voltammetry-scanning electrochemical cell microscopy platform (FSCV-SECCM) in which we are able to track the evolution of adsorbed AQDS as a function of time, in microscopic patches of an HOPG surface and then directly measure the step edge density in the same area. The amount of adsorbed electroactive AQDS is orders of magnitude higher than would be expected if electroactivity was only confined to step edges (even over 5 nm regions of the steps),[26] indicating that most of the electroactivity comes from the graphite basal surface. Moreover, FSCV-SECCM measurements on HOPG of different quality (fractional coverage of steps) show similar responses, indicating that the electron transfer kinetics are in an adiabatic region.[58] Finally, the high electroactivity of the basal surface is further confirmed through SECCM reactive patterning coupled with AFM imaging,[51] where we find high and uniform electrochemical fluxes across the basal surface of HOPG. Significantly, these studies show that the electrochemistry of adsorbed AQDS cannot be used to measure step edges on graphite surfaces and add to an increasing recognition of the intrinsic electroactivity of the graphite basal surface.

EXPERIMENTAL SECTION

Materials and Reagents. All chemicals were used as received. Aqueous solutions were freshly prepared using high-purity Milli-Q reagent water (Millipore Corp.) with resistivity of 18.2 MΩ·cm at 25 °C. ZYA, SPI-1, and SPI-3 grade HOPG were purchased from SPI supplies (West Chester, PA). High-quality, but ungraded, HOPG was kindly provided by Prof. R.L. McCreery (University of Alberta, Canada), originating from Dr. A. Moore, Union Carbide (now GE Advanced Ceramics). This is referred to hereafter as AM grade HOPG. We have shown elsewhere that this material is characterized by a particularly low step edge density.[40] Disodium anthraquinone-2,6-disulfonate and perchloric acid (70%) were purchased from Acros Organics.

Electrode Fabrication and Preparation. All HOPG samples were carefully mounted on a gold-coated (100 nm) silicon wafer with Acheson Electrodag (Agar Scientific, 1415M), and an electrical connection was established by attaching a metal wire to the gold surface. AM, ZYA, SPI-1, and SPI-3 grade HOPG surfaces were freshly prepared for voltammetry measurements by peeling back the top layers of HOPG with Scotch tape, with the cleaving direction maintained to avoid deformation, until the tape was totally covered with HOPG, as routinely done in the literature.[27,37,40,41,49,50,57,59−61] Fresh surfaces of AM HOPG were also revealed by mechanically cleaving with a clean razor blade, inserted perpendicular to the basal plane with a gentle rocking motion until a small piece delaminated spontaneously, as adopted elsewhere.[27,51,62] Both procedures were used for the macroscopic studies of AM grade HOPG, with samples respectively labeled as AM_S and AM_M. For FSCV-SECCM measurements, the AM and SPI-3 samples were prepared via Scotch tape cleavage (AM_S), while for SECCM reactive patterning studies, mechanical cleavage was used for AM (AM_M). As shown in our recent studies, these two cleavage methods produce similar surfaces on AM HOPG.[50]

Macroscale Electrochemistry. Cyclic voltammetry (CV) measurements were carried out with a computer-controlled potentiostat (CH Instruments model 750A, Austin, TX) utilizing a standard three-electrode configuration, where the contacted HOPG sample served as the working electrode, and a silver/silver chloride (Ag/AgCl) electrode and a platinum gauze electrode acted as the reference and counter electrodes, respectively. An O-ring gently placed on the surface with minimal applied force was utilized in order to obtain a well-defined working electrode area (a disc-shaped area with the diameter of 6.2 mm) (Supporting Information, section S1 and Figure

dx.doi.org/10.1021/ja505266d | J. Am. Chem. Soc. 2014, 136, 11444−11451

S1). The solution (10 μM AQDS in 0.1 M $HClO_4$) with a volume of ca. 70 μL was introduced to the surface within a minute of sample cleaving. The reference and counter electrodes were placed into the solution immediately after. All CVs were recorded between 0.1 and −0.5 V vs Ag/AgCl at a scan rate of 0.1 V s^{-1}, after 10 s of solution contact time with the surface, unless otherwise stated.

Ex Situ AFM. AFM topography images of cleaved HOPG substrates and modified surfaces were recorded in air, using a Veeco Enviroscope AFM (Veeco, USA) with a Nanoscope IV controller, operated in tapping mode with silicon nitride tips.

Field-Emission Scanning Electron Microscopy (FE-SEM). FE-SEM images were obtained using a Zeiss SUPRA 55 VP, equipped with in-lens and secondary electron emission detectors.

FSCV and Reactive Patterning with SECCM. FSCV-SECCM measurements were carried out using a dual-channel borosilicate pipet (1.5 mm o.d., 1.2 mm i.d., TGC150-10, Harvard Apparatus) pulled to a sharp taper using a CO_2 laser puller (P-2000, Sutter Instruments), to create an opening of ca. 1 μm diameter, which was subsequently polished to an opening of ca. 18 μm diameter on a polishing wheel. The pipet was silanized using dichlorodimethylsilane to ensure a hydrophobic outer wall, before filling with a solution of 1 μM AQDS in 0.05 M $HClO_4$ and inserting an AgCl-coated Ag wire into each channel to serve as quasi-reference counter electrodes (QRCEs). The order of magnitude lower concentration of AQDS, compared to the macroscopic measurements, ensured that the evolution of AQDS adsorption at the microscale could be followed in real time.

The pipet was mounted on a high-dynamic z-piezoelectric positioner (P-753.3CD LISA, Physik Instrumente) and positioned just above freshly cleaved AM grade HOPG, which was mounted on an xy-piezoelectric stage (P-622.2CL PIHera, Physik Instrumente). A moat of saturated aqueous KCl solution around the substrate was employed to provide a humid atmosphere, preventing evaporation of water from the tip opening. A schematic showing the FSCV-SECCM setup is given in Figure S2. A potential bias (V_2) of 0.05 V was applied between the QRCEs, which gave rise to a conductance current across the meniscus at the end of the pipet (typically ca. 0.1 nA). The pipet approached the HOPG surface (at a rate of 0.1 μm s^{-1}) using the z-piezoelectric positioner, while floating at a potential (V_1) of −0.1 V with respect to ground, so that the substrate experienced a potential of $-(V_1 + 1/2V_2)$, that is, 0.075 V vs Ag/AgCl QRCE, where there was negligible reduction of AQDS (vide infra).

Note that in contrast to SECCM imaging[13,16,41,63,64] with much smaller tips, there was no modulation of the pipet position in these FSCV studies. The DC conductance current (i_{DC}) was adopted as the feedback signal during approach. The approach was immediately halted upon meniscus contact, where an electrochemical cell was formed between the tip and the substrate, as determined by a sudden, dramatic increase in the conductance current (typically by ca. 4 nA). The substrate potential was then maintained (at 0.075 V vs Ag/AgCl) for a predetermined *hold time*, during which AQDS adsorption occurred, before a CV was performed at 100 V s^{-1}, over a substrate potential range of 0.075 to −0.825 V vs Ag/AgCl QRCE. After completion of the first CV, nine subsequent CVs were performed, with the same hold time employed between each of them. This procedure was performed for a wide range of hold times, specifically 50 ms, 100 ms, 250 ms, 0.5 s, 1 s, and 5 s, each at a fresh area of HOPG, requiring the tip to be retracted, moved, and reapproached multiple times, but taking less than ∼30 min in total for all the measurements. High-speed data acquisition at 29 412 points per second (each point the average of 16 equally spaced readings) was achieved using an FPGA card (PCIe-7852R) with a LabVIEW 2013 interface, providing a measured data point roughly every 34 μs.

For SECCM reactive patterning, a dual-channel borosilicate pipet was pulled to a sharp taper (as in the FSCV measurements, but without further polishing), creating two identical pipets: one was used for SECCM and the second imaged with FE-SEM to accurately measure the opening dimensions. The pipet employed was ca. 350 nm in diameter and was again silanized to ensure a hydrophobic outer wall, before being filled with 100 μM AQDS (in 0.1 M $HClO_4$). The AQDS concentration was an order of magnitude higher for the macroscopic measurements, such that the diffusional electrochemical flux at the surface was measured, to complement the FSCV studies, which measured adsorbed material. Ag/AgCl wires served as QRCEs, and the pipet and AM HOPG sample were mounted as outlined for FSCV measurements. In this case, V_2 = 0.3 V and V_1 = 0.25 V with respect to ground, and hence the substrate experienced a potential of −0.4 V vs Ag/AgCl, where diffusion-limited AQDS reduction occurred (vide infra).[65] The pipet approached the HOPG surface, while being oscillated normal to the surface in a sinusoidal fashion (20 nm peak-to-peak amplitude at 233.3 Hz herein) through the z-piezoelectric positioner using a lock-in amplifier (SR830, Stanford Research Instruments). Upon meniscus contact, this oscillation produced an alternating current (i_{AC}) component of the conductance current due to the periodic deformation of the liquid meniscus.[65,66] The AC magnitude was picked out by the lock-in amplifier and used to halt the approach and as a set point to maintain a constant tip-to-substrate separation during imaging and patterning, ensuring that the pipet itself never physically touched the sample. During SECCM experiments the topography, surface electroactivity and conductivity of the solution between the barrels of the probe were recorded simultaneously.[65] For the studies herein, a spiral line pattern covering a length of 560 μm over the HOPG surface at a scan speed of 1 μm s^{-1} was created. The data acquisition rate was 78 points per second (each point the average of 512 readings), corresponding to a pixel size in the scan direction of ca. 13 nm, and resulting in >40 000 individual current measurements.

RESULTS AND DISCUSSION

Impact of HOPG Step Density on Adsorbed Electroactive AQDS. The level of AQDS adsorption from a 10 μM solution (0.1 M $HClO_4$) was first examined at the macroscale employing the O-ring arrangement, on all four grades of HOPG (AM, ZYA, SPI-1, and SPI-3), which vary greatly in surface quality, predominantly in terms of their step edge density (vide infra). These conditions and concentration of AQDS are analogous to those used previously in the assessment of HOPG quality (step edge density) by adsorption.[25,26] Figure 1 shows

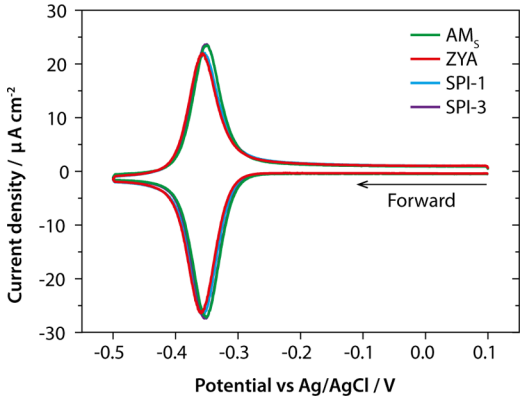

Figure 1. CVs (0.1 V s^{-1}) for the reduction of 10 μM AQDS in 0.1 M $HClO_4$ on four grades of freshly cleaved HOPG: AM_S (Scotch tape cleaved), ZYA, SPI-1, and SPI-3.

representative CVs (0.1 V s^{-1}) for the redox process of adsorbed AQDS on AM_S (green), ZYA (red), SPI-1 (blue), and SPI-3 (purple) grades of HOPG. For each HOPG sample, the CVs are characteristic of an adsorbed species, where the peak separation is nearly zero and the peak width at half-wave height is ∼50 mV, close to the theoretical value of 90.6/n mV, where n is the number of electrons transferred per redox event (i.e., n = 2), for a fast (reversible) process of a surface-bound electroactive species.[67] The adsorbed AQDS surface coverage, Γ_{ads}, was calculated for each sample, as done in previous

dx.doi.org/10.1021/ja505266d | J. Am. Chem. Soc. 2014, 136, 11444−11451

studies,[25,26,34,44] using the charge associated with the reduction wave, obtained via peak integration. Γ_{ads} values were converted to fractional (or percentage) surface coverage values (Θ_{ads}) using a molecular area of 126 Å^2 for AQDS (assuming a flat orientation of the molecule on the surface).[26] Note that, for all HOPG samples, we investigated the time frame over which the maximum AQDS surface coverage was achieved. CVs recorded within ca. 10 s of addition of AQDS solution were the same as those for more extensive periods (of up to 1 h), from which it was concluded that the limit of AQDS adsorption for this concentration must occur within the 10 s time frame of the initial CV.

The mean values of Θ_{ads} obtained for each grade of HOPG, along with corresponding standard deviation, are shown in Figure 2a. For seven repeat measurements on the surfaces of each grade of HOPG, freshly prepared, the following Θ_{ads} were obtained: 29.7 ± 1.6% for AM_S; 29.6 ± 2.4% for AM_M; 29.4 ± 1.2% for ZYA grade; 27.5 ± 1.4% for SPI-1 grade; and 28.0 ± 0.6% for SPI-3 grade HOPG. It is clear that all four grades of HOPG show nearly identical Θ_{ads} values, which are in very close agreement with previous studies that employed high-quality AM grade HOPG.[26] It is also evident that the fractional surface coverage is not affected by the cleaving method (for AM grade). AFM analysis of the step edge coverage for all four grades of HOPG is presented in Figure 2b, highlighting the significant difference in step edge density for the samples. As reported recently,[40,41,49] AM HOPG (with little noticeable difference between Scotch tape and mechanical cleavage) provides the most pristine surface, with the step edge coverage ranging between 0.006 and 0.48% (mean 0.09%), followed by ZYA (range of 0.03−1%, mean 0.3%) and SPI-1 (range of 0.5−3.4%, mean 1.8%), with SPI-3 showing the highest percentage coverage (range of 10−78%, mean 31%), as summarized in Figure 2c. These HOPG samples display increasing step edge density in the order AM, ZYA, SPI-1, and SPI-3, among which the density varies by ∼2 orders of magnitude from the highest quality HOPG (AM) to the lowest quality one (SPI-3). Furthermore, AM and ZYA samples predominantly reveal monolayer and bilayer steps, whereas SPI-1 and SPI-3 show a wide range of step heights with a high proportion of multilayer steps.[40] If the adsorption of AQDS, or indeed its electroactive response, was to be confined only to the step edges, as proposed,[26,27,44] the resulting surface coverages should show a massive difference among the samples investigated. Instead, the Θ_{ads} values for the different grades of HOPG in Figure 2a show negligible variation, strongly indicating that the Θ_{ads} for AQDS is independent of step edge density and dominated by the basal surface. Thus, the electrochemistry of adsorbed AQDS at HOPG is analogous to that seen recently for other reactions: it is dominated by the basal surface.[37,40,41,49−55]

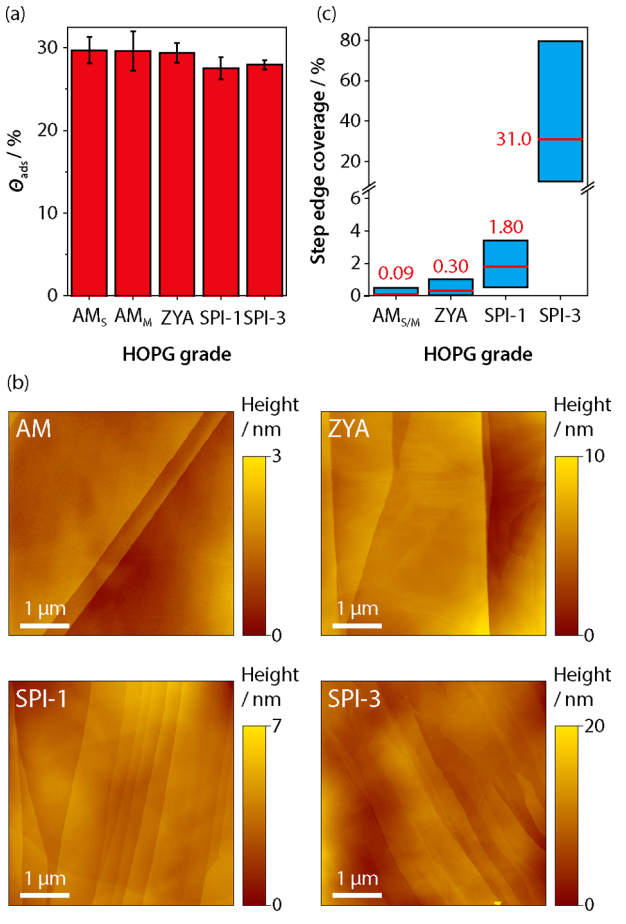

Figure 2. (a) Fractional surface coverages (Θ_{ads}) of AQDS (from 10 μM in bulk solution) in 0.1 M $HClO_4$, from voltammetry at 0.1 V s^{-1}, on different grades of freshly cleaved HOPG: AM_S (Scotch tape cleaved); AM_M (mechanically cleaved); ZYA; SPI-1; and SPI-3. Error bars correspond to one standard deviation of seven measurements on each HOPG grade. (b) AFM images of AM, ZYA, SPI-1, and SPI-3 HOPG samples. (c) Range of step edge coverage on four different grades of basal plane HOPG: AM (AM_S and AM_M); ZYA; SPI-1; SPI-3 (data from refs 40 and 49). The mean value for each data set is marked in red.

Time-Resolved Adsorption Measurements: Structure−Activity Analysis. SECCM allows electrochemical measurements to be performed almost immediately after meniscus contact with the surface.[68] Coupled with the analysis of surface-bound redox species via FSCV, this allowed relatively fast adsorption to be followed in real time. Moreover, by confining the electrochemical cell to the several micrometer scale, via the meniscus footprint, further detailed ex situ topographical analysis could be performed on the *entire area of interest* probed in the electrochemical measurement. This approach allowed a *direct and complete assessment* of the impact of surface properties (notably step edge density) on the electrochemical characteristics in the region of interest. A further attribute of the SECCM setup is that multiple experiments can be performed,[69] each on a fresh, pristine area of the substrate. As such, this provides a powerful platform to thoroughly investigate the process of adsorption at surfaces and is particularly relevant to the present application where the rate of accumulation of redox-active species at the HOPG surface and its dependence on step edge density are of paramount importance.

In the FSCV-SECCM configuration, adsorption began immediately upon contact of the confined solution of AQDS, during a predetermined hold time of the meniscus on the HOPG surface. A CV was then performed at 100 V s^{-1}, in which the surface current (i_{act}) was recorded against substrate potential (E_{surf}), to quantify the level of adsorption after the respective hold time. Upon completion of the FSCV measurement, the same hold time was applied, during which further adsorption occurred, before performing a second FSCV, as illustrated in Figure 3a. This process was repeated a total of 10 times, providing information on the evolution of the level of AQDS adsorption with time at a small area of the surface,

dx.doi.org/10.1021/ja505266d | J. Am. Chem. Soc. 2014, 136, 11444−11451

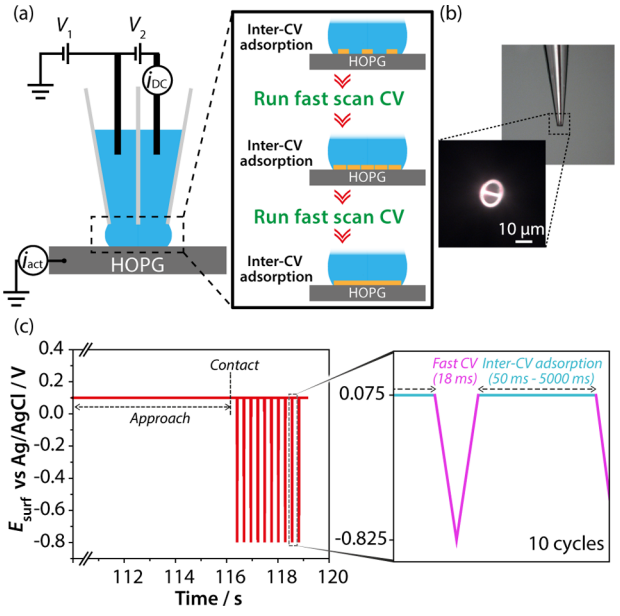

Figure 3. (a) Schematic depicting the process for measuring adsorption on HOPG surfaces via FSCV-SECCM (see text for details). (b) Optical microscope image of a typical tip used in this study, with a diameter of ~18 μm. (c) Potential waveform applied to the substrate during pipet approach and upon meniscus contact, with a zoom showing the potential cycle (repeated 10 times) during adsorption and the FSCV analysis.

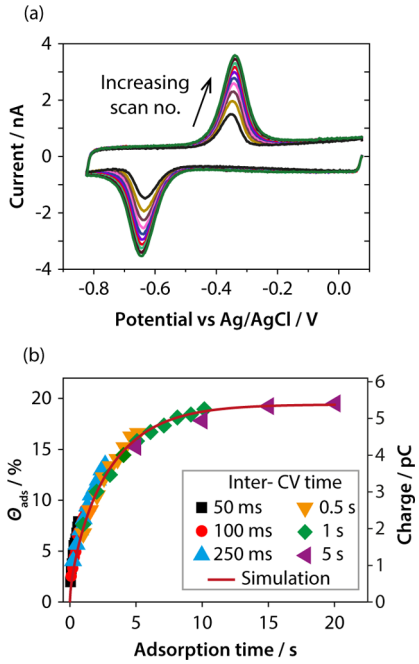

Figure 4. (a) FSCVs (10 in total) for the adsorption of 1 μM AQDS in 0.05 M $HClO_4$, recorded at 250 ms intervals with a scan rate of 100 V s^{-1}, at AM grade HOPG. (b) Observed fractional surface coverage of AQDS calculated from the FSCVs (charge) recorded in different parts of an AM HOPG surface at adsorption time intervals of 50 ms, 100 ms, 250 ms, 0.5 s, 1 s, and 5 s, on AM HOPG. Solid line is the simulated behavior for diffusion-controlled adsorption, with an adsorption constant of 2.4×10^8 cm^3 mol^{-1} (see text and Supporting Information, section S3).

confined by the tip (~18 μm in diameter, Figure 3b). This experiment was performed for a variety of hold times (see Experimental Section) with each carried out at a fresh area of HOPG. The use of a high scan rate during FSCV means that the analysis time (18 ms, defined by the potential scan limits and scan rate) was relatively negligible in comparison to the hold time during which adsorption occurred (Figure 3c), although it is included in the evaluation of the overall adsorption−time curves that are presented below.

A typical example of the voltammograms obtained using the FSCV-SECCM configuration is shown in Figure 4a, where a total of 10 FSCVs were recorded at 250 ms intervals (i.e., a 250 ms hold time) at a single position on the surface. It can be seen that the peak current (i_p) values for the oxidation and reduction waves, corresponding to adsorbed AQDS, increase greatly for the first several FSCVs and then gradually tend to a limiting value with further time. In contrast to the macroscopic measurements (Figure 1), the much higher scan rate employed in FSCV-SECCM leads to a large peak-to-peak separation of the potentials of the oxidation and reduction processes, indicating kinetic influence. This does not affect the evaluation of surface coverage from the integration of the charge under these peaks but opens up interesting possibilities for investigating the impact of step density on kinetics, which we explore briefly below.

As was done for the macroscale experiments, Θ_{ads} was calculated for each recorded FSCV (FSCVs recorded at 1 and 5 s time intervals are provided in Supporting Information, Figure S3). Figure 4b shows Θ_{ads} measured from FSCVs in six regions of the surface against the adsorption time. The significant reproducibility across the wide range of investigated hold times is evident, with a sharp change in the amount of adsorbed AQDS over the first 6 s, which then slowly reaches a maximum value at ca. 10 s. Simulation work was done in order to gain a further understanding of the time scale of the adsorption process (see Supporting Information, section S3). The adsorption process was found to be essentially diffusion-controlled, with an equilibrium adsorption constant of 2.4×10^8 cm^3 mol^{-1}.

Subsequent AFM imaging of the *entire area* covered by each of the FSCV measurements was carried out to allow for a direct comparison between the measured Θ_{ads} and the *actual step edge density*. A typical 15 × 15 μm AFM analysis of an adsorption region after FSCV measurements is shown in Figure 5a, where the total adsorption time was ca. 10 s (1 s hold time × 10 FSCVs), and the Θ_{ads} was measured as ~19%. The AFM image shows adsorption to have occurred over the majority of the working area for which the step edge coverage was ca. 0.091% (expressed as a percentage of the geometric area if the surface was all basal); see also the 3 × 3 μm higher resolution AFM image. Note that the AFM image shows a small spot where a large amount of material is left, which can be attributed to the evaporation of residual solution left behind after retracting the pipet. The important point here is that AFM reveals the precise quantity of step edges compared to basal surface in the area of the experiment.

A comparison of AFM analysis of step edge density and electroactive adsorbed AQDS (expressed as Θ_{ads}) at different hold times and hence different total adsorption times is summarized in Figure 5b. Strikingly, this shows that there is no correlation between step edge density and the level of AQDS adsorption, consistent with macroscopic data presented above (Figure 2). If step edges were the only sites of electroactivity, then in the case of the adsorption after 50 s, where the step

dx.doi.org/10.1021/ja505266d | J. Am. Chem. Soc. 2014, 136, 11444−11451

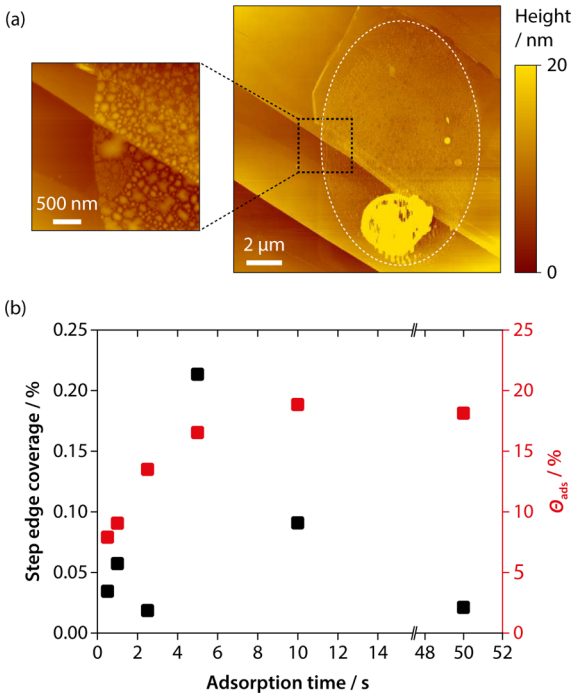

Figure 5. (a) Typical AFM image for the analysis of FSCV adsorption spots on the AM grade HOPG surface taken after a total adsorption time ca. 10 s, with a 3 × 3 μm higher resolution image of the framed area. The approximate droplet footprint is outlined in white. (b) Percentage of step edges found within six adsorption spots where FSCV measurements were made and the observed fractional coverage of electroactive AQDS calculated from the charge at different adsorption times.

edge density is 0.021%, even taking into account possible electronic disorder and partial charges extending up to 5 nm from a step,[26] this would only give a coverage of 0.066%, which is orders of magnitude below the measured Θ_{ads} (ca. 20%). In fact, in all cases in Figure 5b, the observed coverage of electroactive AQDS is orders of magnitude higher than would be expected if there was only electrochemistry of adsorbed AQDS at step edges.

For comparison with the AM sample, further measurements of the adsorption of AQDS at an SPI-3 surface were carried out (see Supporting Information, section S2). These yielded a fractional coverage of ~19% at adsorption equilibrium, very close to the value obtained on AM grade HOPG, further supporting the data obtained from macroscale studies (vide supra). Interestingly, the peak-to-peak separation, ΔE_p (at 100 V s^{-1}), was 344 ± 1 mV (n = 5), closely similar to the value at the AM surface, 341 ± 1 mV (n = 5). Since these two substrates differ in step edge density by more than 2 orders of magnitude, and the SPI-3 grade HOPG has step edge coverage in the range of 10−78%, mean 31% (Figure 2), this indicates clearly that step edges do not influence the reaction kinetics. Furthermore, since the overall DOS on SPI-3 grade HOPG would reasonably be expected to be higher than for AM grade, due to the enhanced DOS at zigzag edges,[45−47] the similarity of the peak-to-peak separation in the FSCV responses for the two HOPG materials suggests that the electroreduction of adsorbed AQDS at HOPG is likely in the adiabatic regime.[58]

SECCM Reactive Patterning. To further examine the sites of AQDS electroactivity on the HOPG surface, SECCM line patterning[49,51] was carried out to map the electrochemical reaction at high spatial resolution and to use the adsorbed AQDS (and the product of the electrochemical reduction) as a place marker for the location of the electrochemical response. As described in the Experimental Section, a much higher concentration of AQDS (100 μM) was used, so that we essentially measured the diffusional flux of reactive AQDS.

Reactive patterning was carried out with an effective surface potential of −0.4 V ($-(V_1 + 1/2V_2)$) vs Ag/AgCl to drive the electrochemical reduction of AQDS, and the line pattern was designed to create a square-spiral line pattern that could be easily recognized and analyzed by a range of complementary techniques. SECCM maps are presented in Figure 6 showing

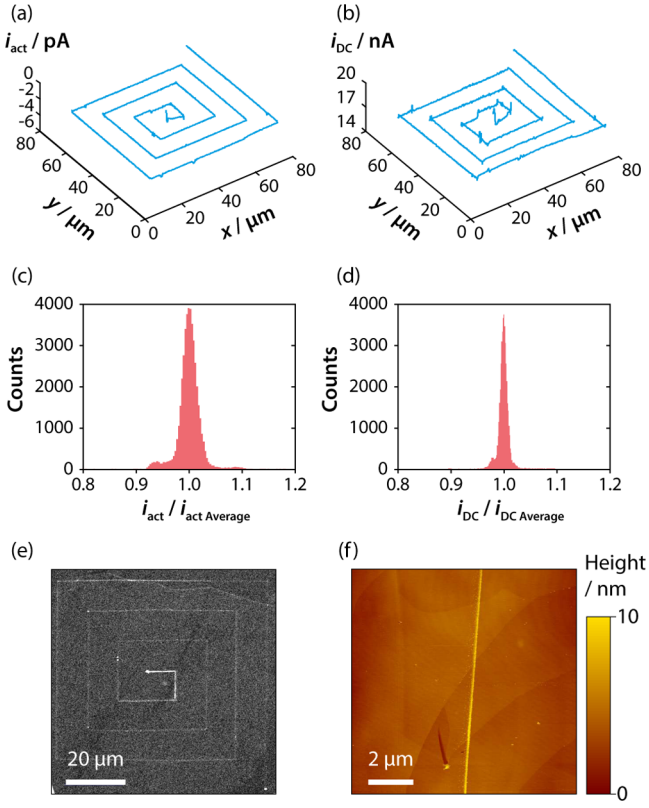

Figure 6. SECCM maps of (a) surface activity (i_{act}) and (b) DC component of conductance current (i_{DC}) for the diffusion-limited reduction of 100 μM AQDS in 0.1 M $HClO_4$ during reactive line patterning on AM HOPG, at a scan speed of 1 μm s^{-1}. Corresponding histograms of the spread of currents are shown in (c) and (d), respectively. (e) FE-SEM image showing the deposited AQDS line pattern. (f) AFM image of part of the pattern.

(a) surface activity (current) and (b) DC conductance current (between the SECCM barrels, which informs on the stability of the meniscus during scanning).[64,70] The spiral pattern, which started in the center, is evident. The SECCM surface activity map shows constant and continuous current values (i_{act}), around −3.25 (±0.1) pA. Given the size of the meniscus, diameter of 350 nm, which can be estimated from the deposited line width obtained from Figure 6f, this corresponds to a flux of ca. 10^{-8} mol cm^{-2} s^{-1}, corresponding to a mass transport coefficient of ca. 0.1 cm s^{-1}, of the magnitude expected in SECCM for a pure diffusion-limited process.[41,65] A histogram showing the spread of surface activity (Figure 6c) for the >40 000 current measurements collected is less than 10%, indicating more or less uniform electroactivity of AQDS throughout the

dx.doi.org/10.1021/ja505266d | J. Am. Chem. Soc. 2014, 136, 11444−11451

adsorption patterning. Figure 6d shows a histogram of i_{DC} values, and the small spread (<3%) highlights the stability of the SECCM meniscus during imaging (further analysis of the alternating current data can be found in Supporting Information, section S4). The deposit formed during the patterning can be seen in the electron micrograph in Figure 6e, a section of which is shown in the AFM image in Figure 6f. It is clear that the electrochemical reactivity data, described above, relate mainly to the basal surface, given the low step density of the AM HOPG surface.[40]

Further AFM characterization is shown in Figure 7a, which is a 3.3 × 3.3 μm AFM image of a section of the line pattern in

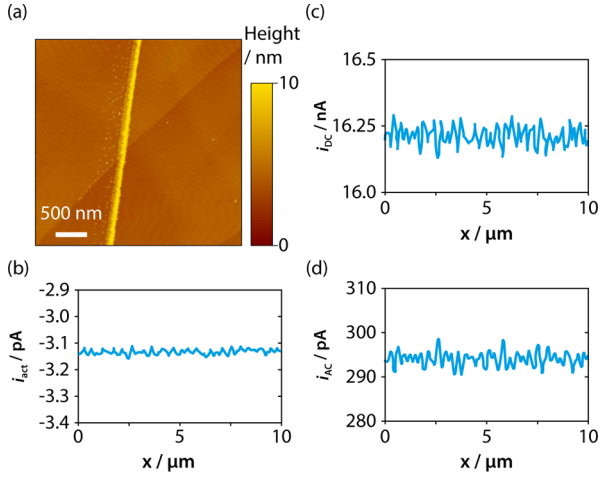

Figure 7. (a) AFM image showing a section of the SECCM line pattern, along with the corresponding SECCM profiles *along the same line* for (b) surface activity (i_{act}), (c) DC component of conductance current (i_{DC}), and (d) AC component of conductance current (i_{AC}), used as a feedback set point.

which the line of adsorbed material travels from a basal terrace over a step edge and onto another basal terrace. The corresponding SECCM maps of (b) surface activity, (c) DC conductance current, and (d) AC feedback current for the same area show that all the currents recorded are stable, and that the electrochemical response is dominated by the basal surface rather than step edges, indicating uniform activity across this area on the spatial resolution of SECCM.

CONCLUSIONS

A new approach for functionalizing and probing the activity of electrode surfaces has been developed, combining the merits of SECCM for high spatial resolution measurements with FSCV to enhance the time scale at which localized surface processes can be probed. These microscale FSCV measurements have allowed the adsorption of AQDS at HOPG to be followed in real time and for the relative kinetics of electron transfer to be compared on different HOPG grades (differing in step edge density by more than 2 orders of magnitude). The adsorption process has been found to be diffusion-controlled, and there is no influence of step edges on the adsorption process or electron transfer kinetics. Importantly, this localized approach allowed direct investigation of surface structure in the region of AQDS adsorption, through AFM imaging of the *entire working area* in which the FSCV measurements were performed. These studies show unambiguously that the rate and amount of AQDS adsorption on HOPG surfaces is independent of the step edge density and dominated by the basal surface. Moreover, the observed coverage of AQDS is orders of magnitude higher than can be accounted for if only AQDS at steps was electrochemically active, which has been a long-standing and widely held view.[38,44] No evidence was found that could indicate preferential electrochemistry of adsorbed AQDS at or around step sites, even taking into account possible electronic disorder (generously) extending up to 5 nm from the step edges.[26] SECCM reactive line patterning was employed to further show that AQDS readily undergoes diffusion-controlled reduction at the basal surface of HOPG, highlighting the high activity of the basal surface.

The data presented herein demonstrate indisputably that AQDS adsorption is not an indicator of step edges present on graphitic surfaces and that there is no correlation between electroactive adsorbed AQDS and step edge coverage. This deduction has been made via a variety of techniques on a range of length scales, from macroscale to nanoscale, with high consistency. Macroscale voltammetry, carried out on a range of surfaces varying greatly in step edge density by ∼2 orders of magnitude, supports the microscale measurements by showing the observed AQDS adsorption to be independent of the step edge density.

The electrochemical activity of HOPG has recently undergone considerable revision. Considered (largely) inert for a long period, various nano/microscale[40,41,49,51−55] and macroscopic studies[37,40,49,50] have shown the HOPG basal plane to support reasonably fast electron transfer for a wide range of reactions. The studies in this paper are important for expanding the range of electrochemical systems that are shown to be facile on the basal surface and because AQDS adsorption has been proposed[26,27] and widely used[25,38,44] as a means of characterizing step edge density, as discussed above. Evidently, this older model and studies which have used it require major reconsideration.

ASSOCIATED CONTENT

Supporting Information

Additional experimental information, simulation, and further SECCM data analysis. This material is available free of charge via the Internet at http://pubs.acs.org.

AUTHOR INFORMATION

Corresponding Author

p.r.unwin@warwick.ac.uk

Notes

The authors declare no competing financial interest.

ACKNOWLEDGMENTS

This work was supported by the European Research Council (ERC-2009-AdG 247143-QUANTIF). G.Z. and A.S.C. acknowledge support by Chancellor's International Scholarships from the University of Warwick. We thank Lubrizol for financial support to P.M.K. We are grateful to EPSRC for a studentship to A.N.P. (Analytical Fund EP/F064861/1e). We also thank Dr. Aleix Güell for helpful comments and advice, and Dr. Alex Colburn for designing and building instrumentation. Some equipment used in this research was obtained through Birmingham Science City with support from Advantage West Midlands and the European Regional Development Fund.

REFERENCES

(1) Ueda, A.; Kato, D.; Kurita, R.; Kamata, T.; Inokuchi, H.; Umemura, S.; Hirono, S.; Niwa, O. *J. Am. Chem. Soc.* **2011**, *133*, 4840.
(2) Güell, A. G.; Meadows, K. E.; Unwin, P. R.; Macpherson, J. V. *Phys. Chem. Chem. Phys.* **2010**, *12*, 10108.
(3) Zhang, L. L.; Zhao, X. S. *Chem. Soc. Rev.* **2009**, *38*, 2520.
(4) Zhou, M.; Zhai, Y.; Dong, S. *Anal. Chem.* **2009**, *81*, 5603.
(5) Pinczewska, A.; Sosna, M.; Bloodworth, S.; Kilburn, J. D.; Bartlett, P. N. *J. Am. Chem. Soc.* **2012**, *134*, 18022.
(6) Wu, Z.; Lv, Y.; Xia, Y.; Webley, P. A.; Zhao, D. *J. Am. Chem. Soc.* **2011**, *134*, 2236.
(7) Singh, Y. S.; Sawarynski, L. E.; Michael, H. M.; Ferrell, R. E.; Murphey-Corb, M. A.; Swain, G. M.; Patel, B. A.; Andrews, A. M. *ACS Chem. Neurosci.* **2010**, *1*, 49.
(8) Patten, H. V.; Lai, S. C. S.; Macpherson, J. V.; Unwin, P. R. *Anal. Chem.* **2012**, *84*, 5427.
(9) McCreery, R. L. *Chem. Rev.* **2008**, *108*, 2646.
(10) Jouikov, V.; Simonet, J. *Langmuir* **2012**, *28*, 931.
(11) Surendranath, Y.; Lutterman, D. A.; Liu, Y.; Nocera, D. G. *J. Am. Chem. Soc.* **2012**, *134*, 6326.
(12) Li, W.; Tan, C.; Lowe, M. A.; Abruña, H. D.; Ralph, D. C. *ACS Nano* **2011**, *5*, 2264.
(13) Güell, A. G.; Ebejer, N.; Snowden, M. E.; Macpherson, J. V.; Unwin, P. R. *J. Am. Chem. Soc.* **2012**, *134*, 7258.
(14) Rodríguez-López, J.; Ritzert, N. L.; Mann, J. A.; Tan, C.; Dichtel, W. R.; Abruña, H. D. *J. Am. Chem. Soc.* **2012**, *134*, 6224.
(15) Yang, W.; Ratinac, K. R.; Ringer, S. P.; Thordarson, P.; Gooding, J. J.; Braet, F. *Angew. Chem., Int. Ed.* **2010**, *49*, 2114.
(16) Lai, S. C. S.; Dudin, P. V.; Macpherson, J. V.; Unwin, P. R. *J. Am. Chem. Soc.* **2011**, *133*, 10744.
(17) Park, J.; Deria, P.; Therien, M. J. *J. Am. Chem. Soc.* **2011**, *133*, 17156.
(18) McCreery, R. L. *Electroanalytical Chemistry*; Dekker: New York, 1991; Vol. *17*.
(19) Sundaram, R. S.; Gómez-Navarro, C.; Balasubramanian, K.; Burghard, M.; Kern, K. *Adv. Mater.* **2008**, *20*, 3050.
(20) Hutton, L.; Newton, M. E.; Unwin, P. R.; Macpherson, J. V. *Anal. Chem.* **2009**, *81*, 1023.
(21) Kutner, W.; Wang, J.; L'her, M.; Buck, R. P. *Pure Appl. Chem.* **1998**, *70*, 1301.
(22) Bahr, J. L.; Yang, J.; Kosynkin, D. V.; Bronikowski, M. J.; Smalley, R. E.; Tour, J. M. *J. Am. Chem. Soc.* **2001**, *123*, 6536.
(23) Safavi, A.; Maleki, N.; Moradlou, O.; Tajabadi, F. *Anal. Biochem.* **2006**, *359*, 224.
(24) McCreery, R. L.; Cline, K. K.; McDermott, C. A.; McDermott, M. T. *Colloids Surf., A* **1994**, *93*, 211.
(25) Xu, J.; Chen, Q.; Swain, G. M. *Anal. Chem.* **1998**, *70*, 3146.
(26) McDermott, M. T.; McCreery, R. L. *Langmuir* **1994**, *10*, 4307.
(27) McDermott, M. T.; Kneten, K.; McCreery, R. L. *J. Phys. Chem.* **1992**, *96*, 3124.
(28) Han, S. W.; Joo, S. W.; Ha, T. H.; Kim, Y.; Kim, K. *J. Phys. Chem. B* **2000**, *104*, 11987.
(29) Soriaga, M. P.; Hubbard, A. T. *J. Am. Chem. Soc.* **1982**, *104*, 2735.
(30) He, P.; Crooks, R. M.; Faulkner, L. R. *J. Phys. Chem.* **1990**, *94*, 1135.
(31) Liu, Y.; Freund, M. S. *Langmuir* **2000**, *16*, 283.
(32) Kano, K.; Uno, B. *Anal. Chem.* **1993**, *65*, 1088.
(33) Zhang, J.; Anson, F. C. *J. Electroanal. Chem.* **1992**, *331*, 945.
(34) Forster, R. J. *Langmuir* **1995**, *11*, 2247.
(35) Forster, R. J. *Anal. Chem.* **1996**, *68*, 3143.
(36) Guin, P. S.; Das, S.; Mandal, P. C. *Int. J. Electrochem.* **2011**, *2011*, 1.
(37) Edwards, M. A.; Bertoncello, P.; Unwin, P. R. *J. Phys. Chem. C* **2009**, *113*, 9218.
(38) McCreery, R. L.; McDermott, M. T. *Anal. Chem.* **2012**, *84*, 2602.
(39) Lee, C.-Y.; Guo, S.-X.; Bond, A. M.; Oldham, K. B. *J. Electroanal. Chem.* **2008**, *615*, 1.
(40) Patel, A. N.; Collignon, M. G.; O'Connell, M. A.; Hung, W. O.; McKelvey, K.; Macpherson, J. V.; Unwin, P. R. *J. Am. Chem. Soc.* **2012**, *134*, 20117.
(41) Lai, S. C. S.; Patel, A. N.; McKelvey, K.; Unwin, P. R. *Angew. Chem., Int. Ed.* **2012**, *51*, 5405.
(42) Robinson, R. S.; Sternitzke, K.; McDermott, M. T.; McCreery, R. L. *J. Electrochem. Soc.* **1991**, *138*, 2412.
(43) Pharr, C. M.; Griffiths, P. R. *Anal. Chem.* **1997**, *69*, 4673.
(44) Ta, T. C.; Kanda, V.; McDermott, M. T. *J. Phys. Chem. B* **1999**, *103*, 1295.
(45) Niimi, Y.; Matsui, T.; Kambara, H.; Tagami, K.; Tsukada, M.; Fukuyama, H. *Phys. Rev. B* **2006**, *73*, 085421.
(46) Kobayashi, Y.; Fukui, K.-i.; Enoki, T.; Kusakabe, K. *Phys. Rev. B* **2006**, *73*, 125415.
(47) Kobayashi, Y.; Kusakabe, K.; Fukui, K.-i.; Enoki, T. *Phys. E* **2006**, *34*, 678.
(48) Nakada, K.; Fujita, M.; Dresselhaus, G.; Dresselhaus, M. S. *Phys. Rev. B* **1996**, *54*, 17954.
(49) Patel, A. N.; Tan, S. Y.; Unwin, P. R. *Chem. Commun.* **2013**, *49*, 8776.
(50) Patel, A. N.; Tan, S. Y.; Miller, T. S.; Macpherson, J. V.; Unwin, P. R. *Anal. Chem.* **2013**, *85*, 11755.
(51) Patel, A. N.; McKelvey, K.; Unwin, P. R. *J. Am. Chem. Soc.* **2012**, *134*, 20246.
(52) Lhenry, S.; Leroux, Y. R.; Hapiot, P. *Anal. Chem.* **2012**, *84*, 7518.
(53) Williams, C. G.; Edwards, M. A.; Colley, A. L.; Macpherson, J. V.; Unwin, P. R. *Anal. Chem.* **2009**, *81*, 2486.
(54) Anne, A.; Cambril, E.; Chovin, A.; Demaille, C.; Goyer, C. *ACS Nano* **2009**, *3*, 2927.
(55) Frederix, P. L.; Bosshart, P. D.; Akiyama, T.; Chami, M.; Gullo, M. R.; Blackstock, J. J.; Dooleweerdt, K.; de Rooij, N. F.; Staufer, U.; Engel, A. *Nanotechnology* **2008**, *19*, 384004.
(56) Davies, T. J.; Hyde, M. E.; Compton, R. G. *Angew. Chem., Int. Ed.* **2005**, *44*, 5121.
(57) Kneten, K. R.; McCreery, R. L. *Anal. Chem.* **1992**, *64*, 2518.
(58) Chen, S.; Liu, Y.; Chen, J. *Chem. Soc. Rev.* **2014**, *43*, 5372.
(59) Bowling, R. J.; Packard, R. T.; McCreery, R. L. *J. Am. Chem. Soc.* **1989**, *111*, 1217.
(60) Rice, R. J.; McCreery, R. L. *Anal. Chem.* **1989**, *61*, 1637.
(61) Cline, K. K.; McDermott, M. T.; McCreery, R. L. *J. Phys. Chem.* **1994**, *98*, 5314.
(62) Chang, H.; Bard, A. J. *Langmuir* **1991**, *7*, 1143.
(63) Ebejer, N.; Schnippering, M.; Colburn, A. W.; Edwards, M. A.; Unwin, P. R. *Anal. Chem.* **2010**, *82*, 9141.
(64) Güell, A. G.; Ebejer, N.; Snowden, M. E.; McKelvey, K.; Macpherson, J. V.; Unwin, P. R. *Proc. Natl. Acad. Sci. U.S.A.* **2012**, *109*, 11487.
(65) Snowden, M. E.; Güell, A. G.; Lai, S. C.; McKelvey, K.; Ebejer, N.; O'Connell, M. A.; Colburn, A. W.; Unwin, P. R. *Anal. Chem.* **2012**, *84*, 2483.
(66) Rodolfa, K. T.; Bruckbauer, A.; Zhou, D.; Korchev, Y. E.; Klenerman, D. *Angew. Chem., Int. Ed.* **2005**, *44*, 6854.
(67) Bard, A. J.; Faulkner, L. R. *Electrochemical Methods: Fundamentals and Applications*, 2nd ed.; John Wiley & Sons: New York, 2001.
(68) Kinnear, S. L.; McKelvey, K.; Snowden, M. E.; Peruffo, M.; Colburn, A. W.; Unwin, P. R. *Langmuir* **2013**, *29*, 15565.
(69) Kirkman, P. M.; Güell, A. G.; Cuharuc, A. S.; Unwin, P. R. *J. Am. Chem. Soc.* **2014**, *136*, 36.
(70) Ebejer, N.; Güell, A. G.; Lai, S. C. S.; McKelvey, K.; Snowden, M. E.; Unwin, P. R. *Annu. Rev. Anal. Chem.* **2013**, *6*, 329.